

## The cytoplasmic domain of the cellulose-synthesizing complex in vascular plants

A. J. Bowling\*, R. M. Brown, Jr.

Section of Molecular Genetics and Microbiology, University of Texas at Austin, Austin, Texas

Received 28 August 2007; Accepted 14 January 2008; Published online 18 August 2008  
© Springer-Verlag 2008

**Summary.** The cytoplasmic domain of the rosette terminal complex has been imaged in situ in patches of plasma membrane isolated from tobacco BY-2 protoplasts. By partially extracting the plasma membrane lipids, cellulose microfibrils were observed through the plasma membrane. Rosette terminal complexes were identified on the basis of their association with the ends of these cellulose microfibrils. The cytoplasmic domain of the rosette terminal complex has been shown to be hexagonal in shape and has been measured to be 45–50 nm in diameter and 30–35 nm tall. These findings demonstrate that the terminal complex does indeed have a substantial cytoplasmic component, and that the hexagonal array observed in the lipid bilayer by freeze fracture is actually only a small part of the overall complex. These findings will allow better modeling of the terminal complex and may facilitate predictions of how many proteins are associated with the rosette terminal complex in vivo.

**Keywords:** Terminal complex; Cellulose synthase; Transmission electron microscopy; Platinum shadowing; Plasma membrane; Tobacco BY-2.

### Introduction

Cellulose is the major structural component of the vascular-plant cell wall. Cellulose is produced by a multisubunit enzyme complex which is thought to produce up to 36 glucan chains both simultaneously and in close proximity to one another. The highly ordered nature of this complex allows the nascent glucan chains to cocrystallize, forming cellulose microfibrils, which are linear and rigid, instead of an amorphous mass of  $\beta$ -glucan.

Large, ordered arrays of cellulose-synthesizing proteins were predicted to exist at the ends of cellulose microfibrils as early as 1958 (Roelofsen 1958). However, it was not

until the advent of the freeze-fracture technique that they were first directly observed (Brown and Montezinos 1976). Due to their association with the termini of cellulose microfibril impressions, they were termed “terminal complexes”. The first terminal complexes discovered were in the green alga *Oocystis apiculata* and were observed to be linear in shape (Brown and Montezinos 1976). Shortly thereafter, rosette terminal complexes were discovered in *Zea mays* (Mueller and Brown 1980) and in the alga *Micrasterias denticulata* (Giddings et al. 1980). Since that time, many researchers have used the freeze-fracture technique to image terminal complexes from a wide variety of sources (Brown 1996).

Rosette terminal complexes from vascular plants are approximately 24 nm in diameter and are composed of six 8 nm subunits (Mueller and Brown 1980, Rudolph and Schnepf 1988, Rudolph et al. 1989, Kimura et al. 1999). The hexagonal rosette structure of the terminal complex in vascular plants is very appealing to many researchers, especially because elementary fibrils (the product of a single terminal complex) were reported to contain 36 glucan chains (Herth 1983). These facts gave rise to the theory that each of the six rosette subunits must synthesize six glucan chains. Several reviews have been published with diagrams indicating that six glucan chains evolve from each of the six members of the rosette (Perrin 2001, Doblin et al. 2002).

Relatively little thought or discussion has been given to the possibility that the part of the rosette terminal complex imaged by freeze fracture is only the hydrophobic, membrane-spanning part of the protein complex, and as such, may only be the exit pore for the nascent glucan chains, and that the real cellulose-synthesizing machinery may be located in the cytoplasm of the cell. One reason for this

\*Present address: A. J. Bowling, Southern Weed Science Research Unit, Agricultural Research Service, U.S. Department of Agriculture, Stoneville, Mississippi, U.S.A.

Correspondence: R. M. Brown, Jr., Section of Molecular Genetics and Microbiology, University of Texas at Austin, Austin, TX 78713, U.S.A.  
E-mail: rmbrown@mail.utexas.edu

neglect may be the simple fact that the cytoplasmic domain of the terminal complex has so rarely been observed (Robards 1969, Kudlicka et al. 1987). In fact, the cellulose synthase enzyme (CesA) has only recently been directly demonstrated to be a part of the rosette terminal complex through immunolabeling of freeze fracture replicas (Kimura et al. 1999).

Although almost all published studies have used freeze fracture, terminal complexes have been imaged, although rarely, in sectioned material. Kudlicka et al. (1987) successfully imaged the linear terminal complexes of the marine alga *Boergesenia forbesii*. Terminal complexes were identified by their direct association with the ends of cellulose microfibrils in grazing sections of regenerating protoplasts. Once some idea of their dimensions and gross morphology in these grazing sections were gained, it became possible for terminal complexes to be located in cross sections of the plasma membrane. The linear terminal complexes were found to extend 30–40 nm into the cytoplasm. This is one of the few studies to date showing the cytoplasmic component of the terminal complex. One earlier study found particles associated with the outer surface of the plasma membrane, which at the time were thought to play a role in cellulose assembly (Robards 1969).

For these reasons, we sought to image the cytoplasmic domain of the rosette terminal complex. In order to maximize the possibility of visualizing the cytoplasmic component of the terminal complex, a technique for the isolation of large areas of the inner surface of the plasma membrane was utilized. The isolation of plasma membrane sheets by binding cells to poly-L-lysine-coated surfaces was first reported by Mazia et al. (1975) for the study of cortical granules in sea urchin eggs, but first applied to plant cells by Marchant (1978) for the study of cortical microtubules in the alga *Mougeotia* sp. Soon after that, cortical microtubules (Van der Valk et al. 1980) and coated vesicles (Van der Valk and Fowke 1981) were found on plasma membrane sheets isolated from tobacco suspension culture cells.

In 1998, Hirai et al. reported the synthesis of  $\beta$ -glucans on plasma membrane sheets isolated from tobacco BY-2 suspension culture cells by repeatedly plunging coverslips with adherent protoplasts into a hypo-osmotic medium. However, transmission electron microscopy of plasma membrane sheets prepared following their mechanical isolation protocol showed that a significant amount of cytoplasmic contamination remained adhered to the plasma membrane sheets, obscuring much of the inner surface of the membrane, where the cytoplasmic domain of the ter-

minal complex would be expected to be. Heuser (2000) advocated the isolation of cell cortices (here called plasma membrane sheets) from animal cells by sonication with a high-power, probe-type sonicator. Unfortunately, this method was found to be excessively destructive to plant cell membranes. However, it was found that sonication of substrates with adherent BY-2 protoplasts in a bath-type sonicator for a controlled amount of time yielded excellent specimens for the observation of the inner surface of the plasma membrane.

## Material and methods

### Cell cultures

*Nicotiana tabacum* Bright Yellow 2 (BY-2) suspension culture cells were grown in modified Linsmaier–Skoog medium (MLS) containing 3% sucrose, 370 mg of *myo*-inositol, 1 mg of thiamine, and 0.2 mg of 2,4-dichlorophenoxyacetic acid per ml, pH 5.7. Cultures were kept in the dark on a gyratory shaker at 60 rpm and 28 °C. Two milliliters of culture medium containing cells were transferred to 100 ml of fresh MLS medium in a flask (volume, 500 ml) every 7 days in order to maintain a high growth rate (Nagata and Kumagai 1999).

### Protoplast production and isolation

BY-2 suspension culture cells were digested in a solution containing 1% (w/v) Onozuka RS cellulase, 0.1% pectolyase, 0.45 M mannitol, and 10 mM morpholineethanesulfonic acid (MES), pH 5.5. This digestion medium was made up as a 3 $\times$  stock and diluted with suspension culture cells in MLS and attached to a rotisserie for 1.5 h at 28 °C. Protoplasts were gently pelleted in a microfuge at approximately 500 g, and the digestion medium was poured off. The protoplasts were resuspended in 1 ml of a heavy solution containing 500 mM sucrose, 1 mM CaCl<sub>2</sub>, and 5 mM MES-KOH, pH 6.0. This solution was transferred to a glass centrifuge tube and 1 ml of a medium-density solution containing 400 mM sucrose, 100 mM D-sorbitol, 1 mM CaCl<sub>2</sub>, and 5 mM MES-KOH, pH 6.0, was carefully layered on top of the protoplasts. A light solution consisting of 500 mM D-sorbitol, 1 mM CaCl<sub>2</sub>, and 5 mM MES-KOH, pH 6.0, was layered on top of the medium solution, and the tube was centrifuged for 5 min at 1000 g in a clinical centrifuge. The interface between the top two layers was collected and diluted in additional light solution and spun again in a microfuge at about 500 g. In order to increase the chances of visualizing cellulose microfibrils, isolated protoplasts were gently pelleted as above and resuspended in MLS plus 0.4 M sorbitol and allowed to regenerate for 15–20 min at 28 °C on a shaker.

### Preparation of "sticky" substrates for the production of membrane sheets

Several different substrates were found to be able to bind protoplasts tightly enough for the production of plasma membrane sheets. Positively charged coverslips were prepared by incubating standard glass coverslips in 50% sulfuric acid plus 5% sodium dichromate for one week to several months. Coverslips were also coated with poly-L-lysine (PLL) by placing a drop of 0.1% PLL onto the surface of a clean glass coverslip for 1–2 min. The PLL was washed off in running deionized water and air-dried. Other glass coverslips were silanized by incubating clean coverslips in a 2% solution of 3-aminopropyl triethoxysilane (APTES) in dry acetone (stored over molecular sieve) for 30 min at room temperature.

Coverslips were rinsed in running deionized water and air-dried. Freshly cleaved mica was also coated with PLL and APTES as described above for glass.

#### Preparation of membrane sheets

Plasma membrane sheets were prepared by a technique modified from those of Heuser (2000) and Hirai et al. (1998). Aliquots of regenerating protoplasts were placed onto "sticky" substrates for 1–2 min. A beaker containing "lysis solution" (50 mM piperazine-N,N'-bis(2-ethanesulfonic acid), pH 7.0; 2 mM MgCl<sub>2</sub>; 5 mM EGTA) was placed into a bath-type sonicator and the sonicator was switched on. The plasma membrane sheets were generated by plunging substrates (coverslips or mica squares) with bound protoplasts into the beaker of lysis solution in the sonicator. The coverslip was vigorously moved up and down in the lysis solution, with the sonicator running, for 10–20 s and then plunged immediately into a fixative solution of 4% formaldehyde, 1% glutaraldehyde, 50 mM cacodylate (pH about 7.4), and 2.5 mM CaCl<sub>2</sub>. Membrane sheets were fixed for 30 min to 1 h at room temperature. Some plasma membrane sheets were postfixed in 1% OsO<sub>4</sub> (in distilled deionized water) for 1 h at room temperature. Some samples were dehydrated after osmication, and some were tertiary fixed in 1% uranyl acetate (in distilled deionized water) for 1 h at room temperature. After all fixative steps, the specimens were rinsed several times with distilled deionized water. Specimens were dehydrated in a graded series of ethanol (70%, 95%, and absolute for 5 min each) followed by hexamethyldisilazane (HMDS) for 5 min and then air-dried.

#### Replication of membrane sheets

Substrates with attached membrane sheets were rotary shadowed in an Edwards E306A high-vacuum evaporator. Four centimeters of 0.1 mm diameter platinum wire was resistance-evaporated from a graphite electrode located 8–10 cm above the specimen. Specimens were rotated at full speed (about 5 revolutions per second) and 75° tilt (15° from vertical). Platinum was evaporated below  $2 \times 10^{-5}$  Torr (ca.  $3 \times 10^{-3}$  Pa) with the rough pump off to minimize vibrations. Specimens were backed with carbon at about 10° from horizontal, at full speed rotation, for 8–10 s.

Replicas were floated off of the glass by immersing in full strength (47%) hydrofluoric acid. Replicas were collected from the surface of the hydrofluoric acid with a glass rod and floated onto glass-distilled water. Specimens were rinsed on glass-distilled water 3 times and then cleaned with sulfochromic acid (5% sodium dichromate in 50% sulfuric acid) for 10–60 min. Specimens were then rinsed on three changes of glass-distilled water and collected on Formvar-covered, 75-mesh copper grids and examined in a Philips EM420 transmission electron microscope (TEM) at 100 kV. Digital images were captured with a Gatan Bioscan camera.

#### Creation of 3-dimensional anaglyphs

The goniometer stage of the TEM was tilted +5° and -5° (10° total) and two images were captured. The two images were pasted into different layers using the GNU Image Manipulation Program (the GIMP) v 2.2, the opacity of the overlaying images was decreased, and particles from the background were carefully matched. The images were then cropped to be exactly the same size (areas where the two images did not overlap were cut off). The images were converted from grayscale to RGB. The blue and green channels were deleted from the left image (to generate a red image) and the red channel was deleted from the right image (to generate a blue-green image). Thus, when wearing red-blue 3-D glasses, each eye sees only one of the two images, which, because the images were taken at different tilt angles, the human brain interprets as 3-D information.

## Results

### Ultrastructure of plasma membrane sheets prepared by sonication

When protoplasts are attached to a polylysine-coated coverslip and then sonicated, patches of plasma membrane

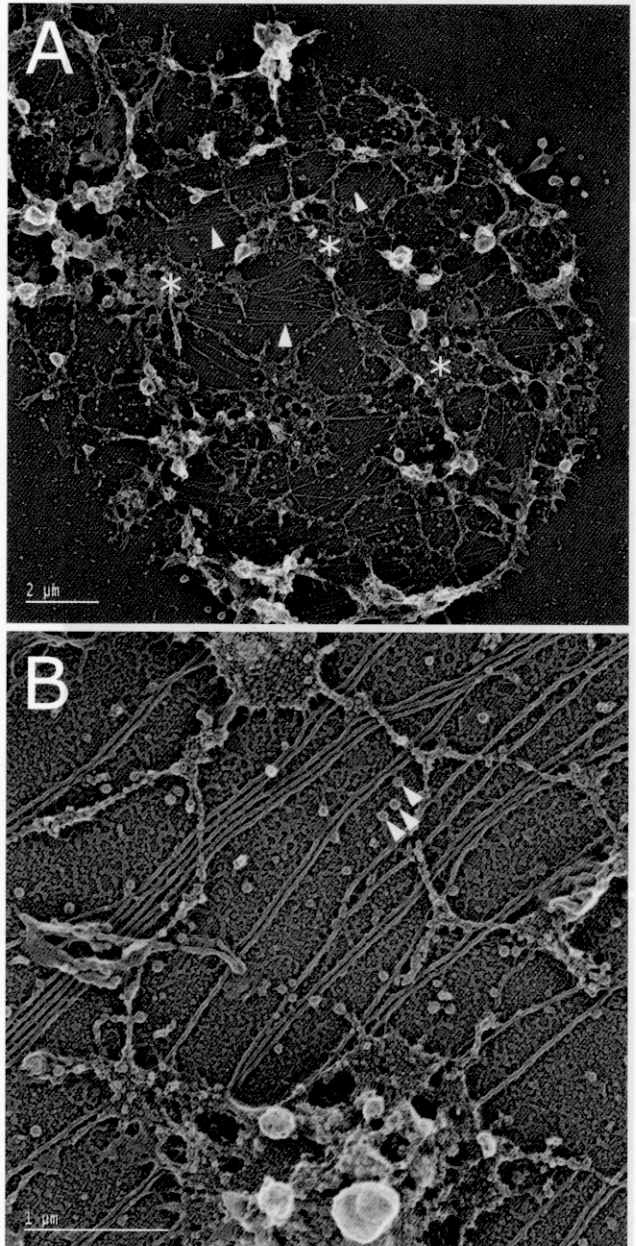
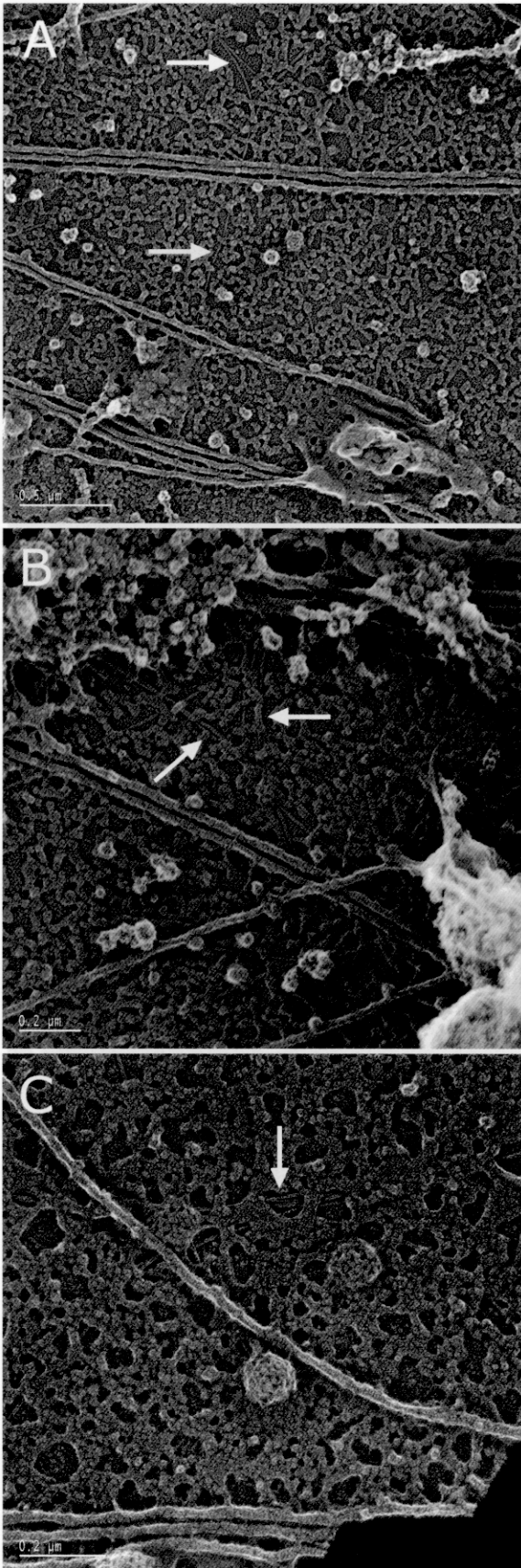


**Fig. 1 A, B.** Ultrastructure of cell cortices prepared by sonication. **A** Plasma membrane sheet at low magnification. Note the presence of parallel microtubules (arrowheads) and an extensive cortical endoplasmic reticulum network (asterisks). Bar: 2 µm. **B** At higher magnification, clathrin-coated vesicles (arrowheads) can just be discerned budding off the membrane and cross-links can be seen between the microtubules of a bundle. Here again, a network of endoplasmic reticulum can be seen just interior to the cortical microtubules. Bar: 1 µm



remain attached, cytoplasmic side up. What remains attached to the sticky substrate after sonication is less than a cell ghost, which retains much of the cytoplasmic components of the cell, and so the term “plasma membrane sheet” is used in this manuscript. Plasma membrane sheets isolated from regenerating BY-2 protoplasts frequently display a large number of parallel, bundled cortical microtubules (Fig. 1 A, B). These plasma membrane sheets also have what appears to be an extended system of membrane-bound, cortical rough endoplasmic reticulum (RER) which passes over (toward the interior of the cell) the plasma membrane-bound microtubules. The cortical RER system appears to be organized into a network of hubs connected by elongated bridges. While all or most of the bundles of cortical microtubules attached to a given plasma membrane sheet appear to be co-aligned, the cortical RER system does not appear to be oriented in one specific direction. Clathrin-coated pits and vesicles can just be discerned in Fig. 1 B. Furthermore, at this magnification, the surface of the plasma membrane itself can be seen to have aggregated into a reticulated network.

At higher magnification (Fig. 2), cellulose microfibrils can be visualized under the plasma membrane due to the extensive network of holes present in the membrane. An anaglyph of these microfibrils running behind the plasma membrane is shown in Fig. 4 C. Also, in Fig. 2 C, patches of clathrin can be seen associated with the plasma membrane.

In order to determine if extraction of membrane lipids was responsible for the reticulated appearance of plasma membrane sheets, some aldehyde-fixed plasma membrane sheets were postfixed with osmium tetroxide and uranyl acetate. Following this additional fixation regimen, the plasma membrane surface displays none of the reticulate structure common to aldehyde-fixed plasma membrane sheets (Fig. 3). Instead of being totally smooth, a large number of small bumps can be seen to cover a large percentage of the plasma membrane surface. These particles could represent trans-membrane or membrane-associated proteins that protrude through the bimolecular leaflet. Some folds can also be seen in these sheets, possibly occurring when the (nearly) spherical protoplast binds to the flat glass surface (Fig. 3 A). The structure of clathrin-

**Fig. 2A–C.** Cellulose microfibrils are visible underneath extracted plasma membrane sheets attached to polylysine-coated substrates. The partial extraction of membrane lipids that occurs during specimen dehydration in ethanol allows the imaging of cellulose microfibrils (arrows) through holes in the plasma membrane sheets. Bar: A, 0.5  $\mu\text{m}$ ; B and C, 0.2  $\mu\text{m}$ .

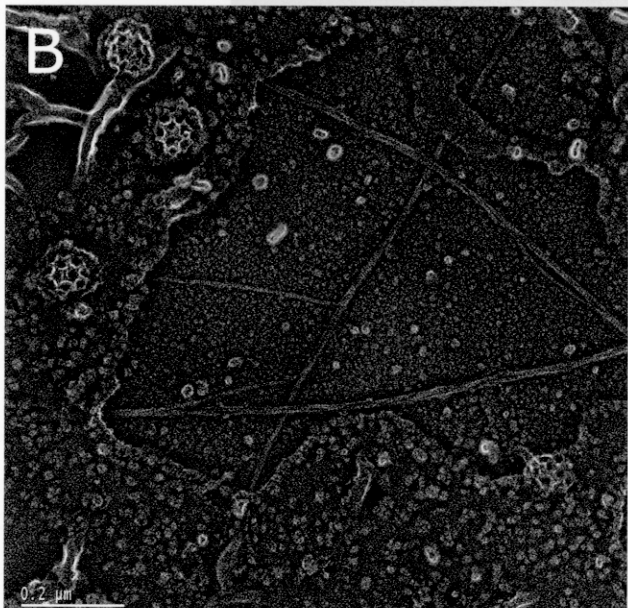
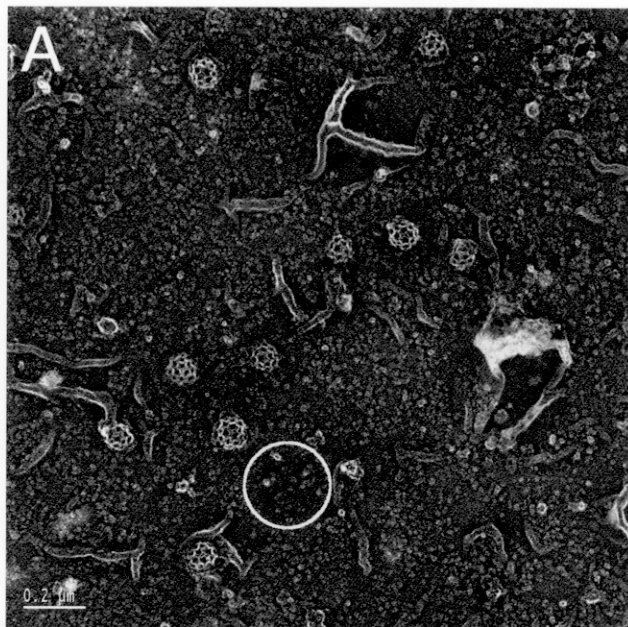


**Fig. 3 A, B.** Effect of lipid fixatives on membrane sheet ultrastructure. **A** Membrane sheet fixed in aldehyde, osmium tetroxide, and uranyl acetate. The surface of the membrane looks totally intact. The presence of granular particles bound to the membrane can be seen. The structure of the clathrin-coated vesicles can be seen to be superior to that seen in membrane sheets fixed with aldehyde only (e.g., Fig. 2). Cellulose microfibrils, however, cannot be seen under these membrane sheets. **B** Cellulose microfibrils can be seen in a hole torn through the plasma membrane sheet, demonstrating that cellulose microfibrils are indeed present under the membrane sheet even though they cannot be detected. Bars: 0.2  $\mu\text{m}$

coated pits and vesicles is markedly improved from aldehyde-only fixed specimens. This is most likely due to the increased preservation of the membrane lipids on which they self-assemble.

One consequence of this improved preservation of the plasma membrane ultrastructure is the greatly reduced ability to detect the presence of cellulose microfibrils under the plasma membrane sheets. Their presence can be confirmed both around the periphery of the cell as well as through “windows” that are occasionally seen torn through the plasma membranes (Fig. 3B). Where the cellulose microfibrils pass under the plasma membrane sheet, there is no corresponding visible sign of a clear impression on the interior surface of the sheet.

#### *Three-dimensional analysis of plasma membrane sheet ultrastructure*

In order to better understand the three-dimensional nature of the membrane sheets, anaglyphs were made by tilting the goniometer stage of the TEM  $+5^\circ$  and  $-5^\circ$  ( $10^\circ$  total). These images must be viewed with red–blue (or red–cyan) glasses, with the red lens over the left eye. In Fig. 4A, a bundle of plasma membrane-bound cortical microtubules can be seen along with several membrane-bound clathrin-coated vesicles. On the left, a piece of cortical RER can be seen lying on top of a microtubule and spreading over an area of the plasma membrane. The surface of the plasma membrane appears pebbled. In some places, many clathrin-coated vesicles appear to bud off from a small region (Fig. 4C). Occasionally, as the cell body tears away, the cellulose microfibrils which were wrapped around the cell tear through the delicate plasma membrane (Fig. 4C, lower right).

Many highly oriented plasma membrane-bound microtubules exist in the cell cortex of BY-2 protoplasts and remain bound to the plasma membrane after membrane sheet isolation. Just interior to this plasma membrane-bound microtubule system is a large network of RER (Fig. 4A, B, D). The specimen shown in Fig. 4D was postfixed with osmium tetroxide and uranyl acetate (the same as for the sheets shown in Fig. 3). For this reason, the structure of the plasma membrane surface as well as the clathrin-coated vesicles is markedly different from that in other images in Fig. 4. Although the cortical RER is directly adjacent to the cortical microtubules, they appear to be unconnected.

#### *Evidence to support the presence of a cytoplasmic domain associated with rosette cellulose-synthesizing complexes of tobacco BY-2 cells*

The cellulose microfibrils present under extracted plasma membrane sheets could sometimes be tracked back to

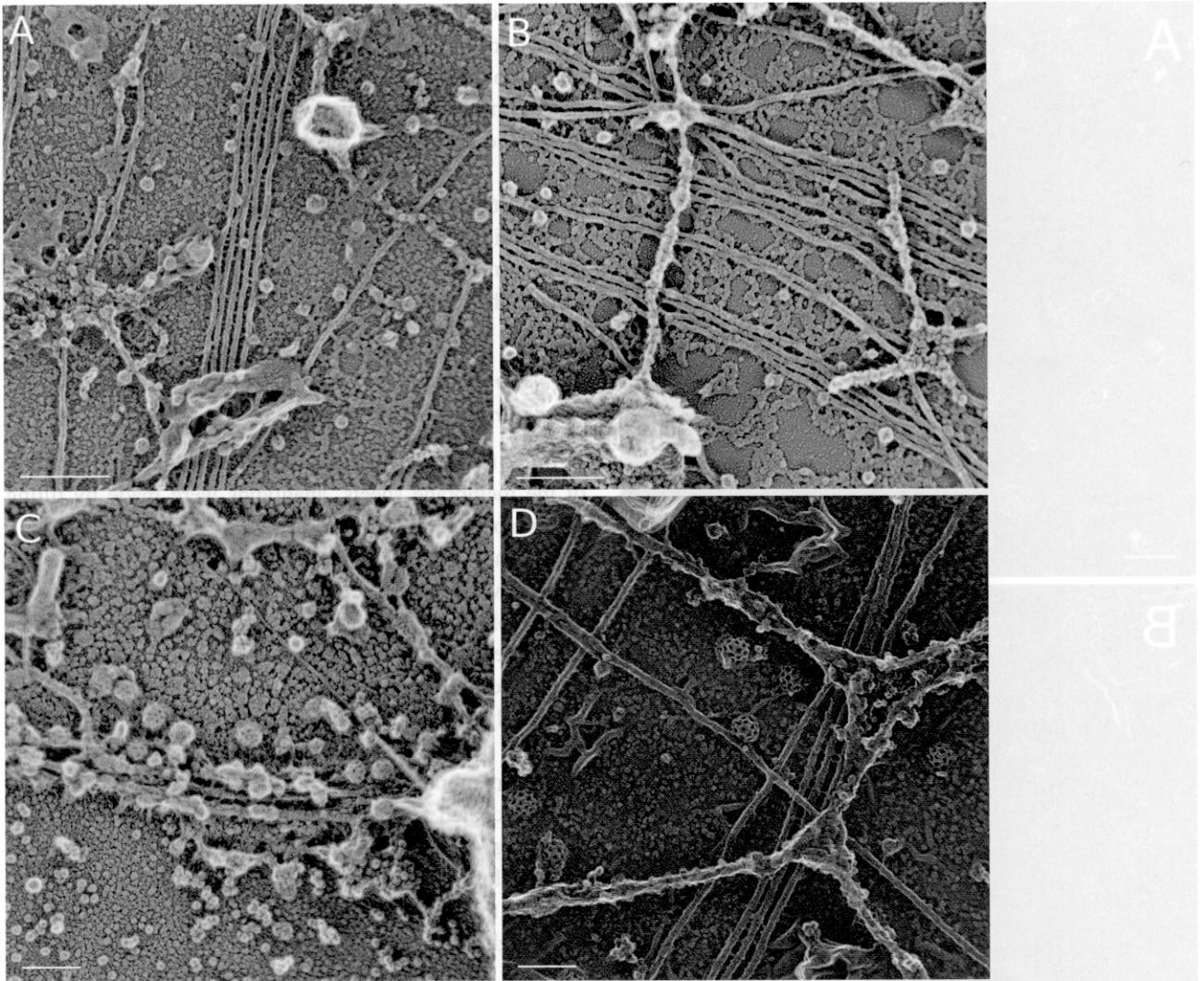


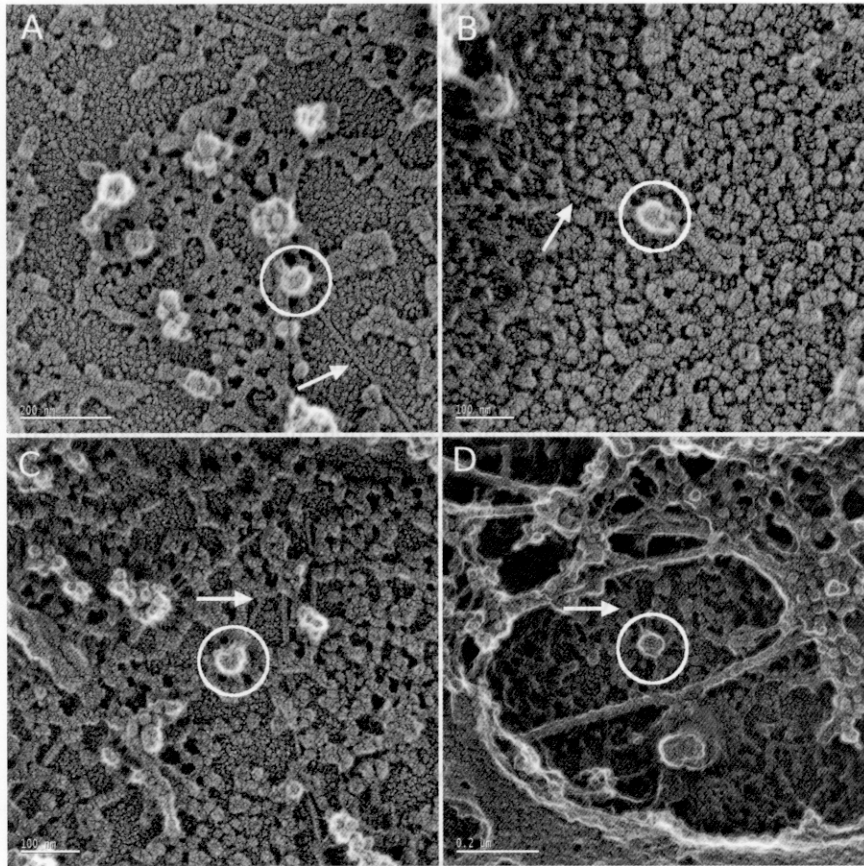
**Fig. 4A–D.** Three-dimensional analysis of BY-2 membrane sheets. **A** Relatively low-magnification image showing a bundle of five plasma membrane-bound cortical microtubules. Clathrin-coated vesicles can be seen bound to the membrane surface. Cross-links can be seen between the members of the microtubule bundle. **B** Many highly oriented, plasma membrane-bound cortical microtubules are visible here. Just above the plasma membrane-bound microtubules is a network of RER. These structures can be easily distinguished by the large number of ribosomes bound all over their exterior. **C** A row of clathrin-coated vesicles appears ready to bud off the membrane in this image of the edge of a membrane sheet. A cellulose microfibril can be seen on the lower right side of the image. It has torn through the soft sheet. **D** As in Fig. 3, this plasma membrane sheet has been postfixed with osmium tetroxide and uranyl acetate, greatly enhancing the preservation of the membrane itself as well as clathrin-coated structures. Plasma membrane-bound microtubules can be seen passing under the cortical RER network. Several clathrin-coated pits and vesicles are apparent attached to the membrane surface between the microtubule systems. Bars: A and B, 0.5  $\mu\text{m}$ ; C and D, 0.2  $\mu\text{m}$

their ends. Globular particles were found associated with these ends. Some of these particles display a marked hexagonal geometry (Fig. 5A–D).

Markham rotational analysis (Markham et al. 1963) was performed on several putative hexagonal terminal complexes to confirm the presence of a hexagonal shape (Fig. 6). Each terminal complex image was copied, rotated  $60^\circ$ , and added to the previous image. The reinforcement of the hexagonal shape by adding images rotated by  $60^\circ$  confirms that these particles are indeed truly hexagonal in shape. When the images were rotated at other an-

gles besides  $60^\circ$ , the final shape averaged into a circle (data not shown).

Hexagonal particles were also seen that were not connected to cellulose microfibrils (Fig. 7). These particles have the same size and shape as the hexagonal particles seen attached to cellulose microfibril termini (Fig. 8). Due to the fact that these plasma membrane sheets were isolated from actively regenerating protoplasts, it is likely that these hexagonal particles are newly inserted terminal complexes that have not yet initiated cellulose microfibril assembly. Another possible interpretation is that these par-



icles are the result of the cellulose mi  
dissociated from the terminal comp  
ing the process of adhering the pro  
state. One hundred and fourteen m  
over 38 unique hexagonal particles w  
cited microfibers yielded an average  
point) of  $54.7 \pm 6.4$  nm.

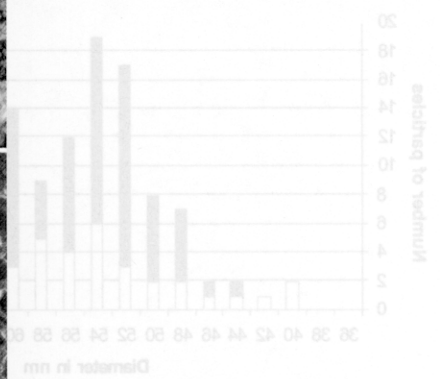


**Fig. 5 A-D.** Hexagonal structures can be seen attached directly to the ends of cellulose microfibrils. The cytoplasmic domains of rosette terminal complexes (circled) can be identified by their association with the termini of cellulose microfibrils (arrows). Bar: A, 200 nm; B and C, 100 nm; D, 0.2  $\mu$ m

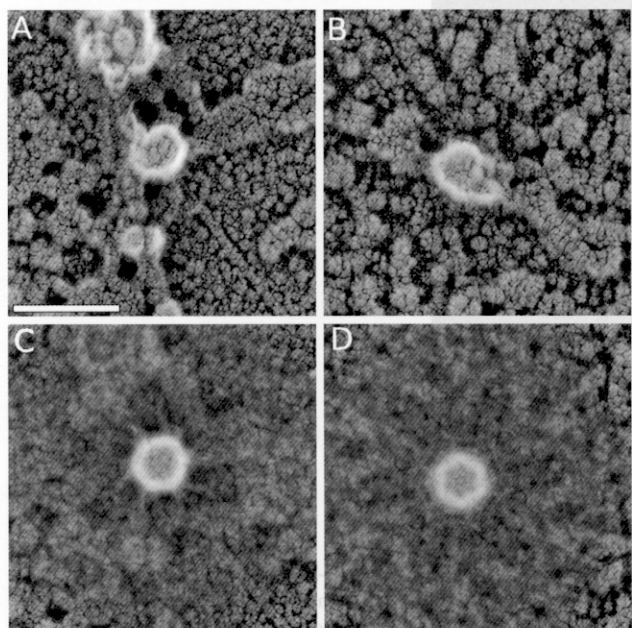


**Fig. 6 A-D.** Markham rotational analysis of two significantly hexagonal terminal complexes. **A** and **B** Two hexagonal terminal complexes. **C** and **D** Markham rotational analysis of **A** and **B**. Images were rotated in  $60^\circ$  increments and added back to the original image. Rotation of images by anything other than  $60^\circ$  causes averaging out of the hexagonal shape into a circular shape (data not shown). Bar: 100 nm

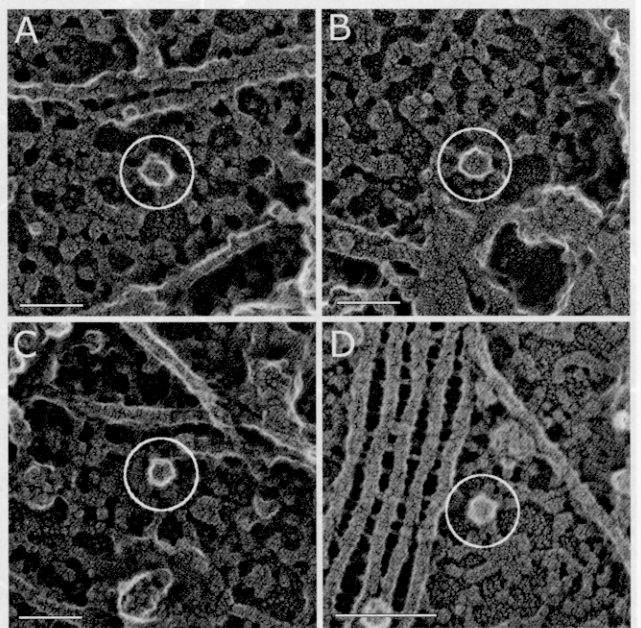


**Fig. 7 A-D.** Hexagonal particles not associated with cellulose microfibrils. **A-C** Hexagonal particles found on the inner surface of the plasma membrane without apparent association with cellulose microfibril termini. **D** Hexagonal particle not associated with a microfibril terminus, but in close proximity to a bundle of microtubules. The height of the hexagonal cytoplasmic domain can be estimated to be 35 nm on the basis of a comparison with these juxtaposed cortical microtubules. Bars: 200 nm

ticles are the result of the cellulose microfibrils becoming disassociated from the terminal complexes, perhaps during the process of adhering the protoplasts to the substrate. One hundred and fourteen measurements made over 38 unique hexagonal particles with and without associated microfibrils yielded an average diameter (point-to-point) of  $54.7 \pm 6.4$  nm.

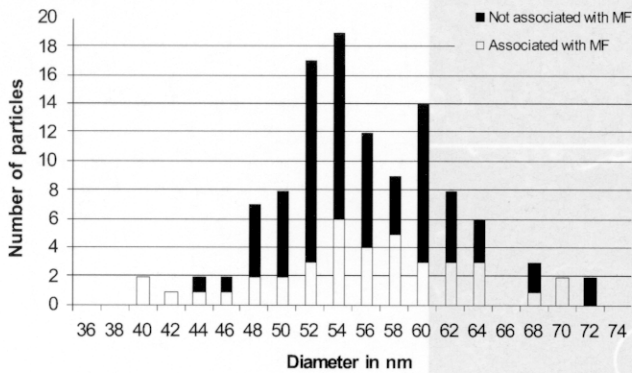


**Fig. 8.** Size distribution of hexagonal terminal complexes. A high degree of correlation exists between the diameters of hexagonal particles associated with cellulose microfibril termini and hexagonal particles not associated with cellulose microfibril termini.

In Fig. 7D, a hexagonal particle approximately 50 nm in diameter can be seen adjacent to a bundle of microtubules. The microtubules in this image have a range of diameters between 26 and 28 nm. Despite this variation, their average diameter is in accordance with the known diameter of microtubules obtained through X-ray and electron crystallography (Nogales et al. 1999, Amos 2000). The microtubules in this image, being isolated from a living cell, almost certainly have many types of microtubule-associated proteins bound to them, thus increasing their apparent diameters and resulting in the observed irregularity in their diameters. Since microtubules are circular in cross section, the height of these microtubules is probably very similar to their width (26–28 nm). The hexagonal particle shown in Fig. 7D appears slightly taller than the neighboring microtubule, i.e., approximately 30–35 nm tall.

Occasionally, cellulose microfibrils terminate in non-hexagonal structures (Fig. 9), which are frequently composed of many small objects (Fig. 9C, D). These non-hexagonal structures have been tentatively identified as terminal complexes in the process of being inactivated and broken down, possibly by proteolytic mechanisms

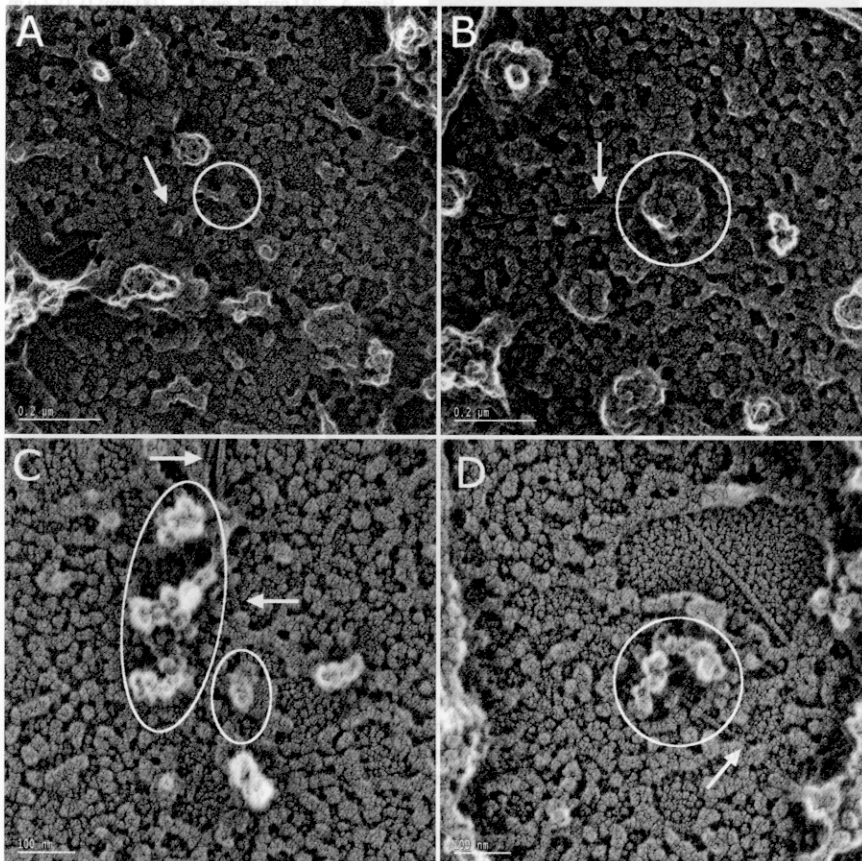


**Fig. 9 A–D.** Nonhexagonal particles associated with the ends of cellulose microfibrils. **A** Cellulose microfibril that appears to end with no conspicuous particle associated with it. **B** Cellulose microfibril ends with a large, amorphous structure. **C** and **D** Three different cellulose microfibril termini, each with a varying number of small, roughly spherical particles in the immediate vicinity. Bar: A and B, 0.2  $\mu$ m; C and D, 100 nm



(Nakashima et al. 2003). Therefore, these small substructures may in fact be the individual cellulose synthase subunits that compose the terminal complex and/or accessory proteins associated with the terminal complex at the time of its inactivation.

## Discussion

### *The cytoplasmic domain of the terminal complex*

In order to visualize the cytoplasmic region of the rosette terminal complex, large regions of plasma membrane with the cytoplasmic face exposed were isolated. These patches of plasma membrane were cleaned of adhering cytoplasmic material by a brief sonication. In order to ensure the best preservation of cellular ultrastructure, the plasma membrane sheets went from intact protoplasts, through lysis and sonication, and into fixative in less than 10 s. The isolation of large regions of plasma membrane free of any covering layer of cytoplasmic proteins has made possible the visualization of the cytoplasmic domain of the vascular-plant cellulose-synthesizing rosette terminal complex. Terminal complexes were positively identified by their location at the end of a cellulose microfibril. The relatively small standard deviation in the measured size of hexagonal terminal complexes seems to indicate that these are in fact intact and complete terminal complexes and not an intermediate stage in terminal complex maturation.

In terms of absolute dimensions, it should be noted that an enlargement of the apparent diameters of terminal complexes is due to the presence of the metal coating itself as well as the accretion of a metal "cap" during shadowing. On the basis of the mass of platinum evaporated, the angle of the specimen, and the distance to the specimen, the thickness of the platinum-carbon film has been calculated to be 2.5 nm (Bradley 1965, Willison and Rowe 1980). Furthermore, the accretion of a metal cap by particulate specimens shadowed at high angles is usually less than 5 nm (Willison and Rowe 1980). This is in agreement with the observed amount of broadening of microtubule diameters, from which the thickness of the shadowing film has been independently estimated to be 2–2.5 nm. Therefore, approximately 4–5 nm (the thickness of the film) and 1–5 nm (from the "cap" material) should be subtracted from the values measured on the replica to estimate the "true" size of the terminal complex. The expected diameter of the cytoplasmic domain of the terminal complex, therefore, is approximately 45–50 nm (point to point). This is roughly twice the 25 nm diameter reported for rosette terminal complexes seen by freeze fracture.

Estimation of the height of shadowed structures can be done in several ways. The estimation of the height of particles by measuring the shadow length in unidirectionally shadowed samples is only possible on very flat surfaces (e.g., purified molecules on mica or glass). Due to the fact that the surface of the plasma membrane is so uneven following the ethanol extraction, unidirectional shadowing for the estimation of particle height is of limited value. It is also theoretically possible to measure the height of shadowed particles by measuring the height of the particles at high tilt angles. Here again, the unevenness of the partially extracted plasma membrane makes this measurement unreliable. Furthermore, the height of the particles in these images will be smaller than their true height due to the flattening effect of drying biological specimens for metal shadowing. Despite these facts, some idea of the height of the rosette terminal complexes has been obtained through comparison of the apparent height of the cytoplasmic component of the terminal complexes with other structures present on the plasma membrane sheet of known size, such as microtubules, ribosomes, and the cellulose microfibrils themselves.

### *Other methods to aid in the identification of rosette terminal complexes*

Besides their association with the ends of cellulose microfibrils, the identification of terminal complexes was attempted by other complementary techniques. The PATAG method of Roland and Vian (1991) was used to deposit silver particles along the cellulose microfibrils, thus identifying them as cellulose as well as facilitating the tracking of the microfibrils to their termini. Unfortunately, this method did not work on our specimens. Plasma membrane sheets are generated with the cellulose microfibrils trapped between the membrane and the glass. PATAG reagents applied from the cytoplasmic sheets do not have access to the cellulose microfibrils (the holes are formed during dehydration and extraction with ethanol). After the coverslips had been dissolved, the replicas were floated in the PATAG reagents, but the cellulose microfibrils may have been degraded or altered by their immersion in hydrofluoric acid. Cellulase-colloidal gold conjugates were also used in an attempt to identify the cellulose microfibrils. This did not work either. It is likely that residual cellulase in the cellulase-gold solution very rapidly degrades the (approximately) 36-glucan chain, single-terminal complex-product microfibrils present in these specimens. We also attempted to localize the terminal complexes with anti-CesA antibodies, similar to the work of Kimura et al.

(1999). We found that the blocking agents required for background-free localization of CesaA antigens with this antibody totally obscured the nanometer-scale features of the plasma membrane surface, such as the 2–4 nm cellulose microfibrils and the hexagonal shape of the rosette terminal complexes.

Recently, Paredez et al. (2006) have shown that treatment of cells with 2,6-dichlorobenzonitrile (DCB) causes a buildup of fluorescently tagged CesaA-containing structures on the plasma membrane. Perhaps this technique could be used with BY-2 protoplasts to increase the number of terminal complexes available for analysis on a given plasma membrane sheet. An increase in the number of terminal complexes following treatment with DCB would provide further evidence that these structures are the same CesaA-containing structures visualized by Paredez et al. However, when BY-2 protoplasts were treated with DCB, they were found to synthesize an amorphous, nonfibrillar product (data not shown). For this reason, and because the exact effect of DCB on the structure of the cytoplasmic domain of the terminal complex is currently unknown, these experiments were not pursued further until a method of labeling the terminal complex besides being attached to a microfibril is discovered. Furthermore, protoplasts could be treated with isoxaben, which would cause the disappearance of hexagonal terminal complexes from the plasma membrane. Unfortunately, the occurrence of visible terminal complexes is already so rare that their disappearance may be unconvincing.

#### *Comparison of cytoplasmic domains with terminal complexes observed by freeze fracture and sectioning*

Rosette terminal complexes from vascular plants are known to be composed of six subunits. These rosettes are integral membrane proteins. Furthermore, the size and shape of the rosette terminal complexes seen in vascular plants by freeze fracture is constant (Brown 1996). Freeze-fracture micrographs show the presence of rosette structures on the P fracture face. Since the P fracture face is the cytoplasmic leaflet of the plasma membrane bilayer, there are no cellulose microfibrils present. The rosette terminal complexes are therefore identified by their association with “microfibril impressions” (Brown and Montezinos 1976, Mueller and Brown 1980). The hexagonally shaped terminal complexes seen in this study are directly connected to cellulose microfibrils. This mirrors what has long been observed indirectly on freeze-fracture micrographs.

The isolation of plasma membrane sheets allows the observation of very large areas of what would be referred to as the PS face in freeze fracture terminology (Branton et al. 1975). Observation of this face in specimens prepared by freeze fracture is very rare. Thus, for the observation of the cytoplasmic domain of transmembrane protein complexes, the current plasma membrane sheet technique is much preferred and more useful.

Terminal complexes have only rarely been seen in sectioned material. One reason for this is probably that the rosette terminal complex is only a fraction of the size of the extremely large linear terminal complexes found in *B. forbesii* (Kudlicka et al. 1987). Also, in cross section, rosette terminal complexes would not have the distinctive hexagonal shape seen in the en face view seen in this study, nor would they be able to be correlated with the ends of microfibrils. However, now that the cytoplasmic domain of the rosette terminal complex has been shown to have a distinct hexagonal shape, perhaps terminal complexes can be identified in grazing sections. This might be an excellent use for the new GFP-CesaA model system recently created by Paredez et al. (2006). Also, because blocking reagents do not occlude ultrastructure in plastic sections, perhaps immunolabeling of CesaA in grazing sections would be possible.

The linear terminal complexes of *B. forbesii* have been measured to extend 35 nm from the exoplasmic face to the endoplasmic face (Kudlicka et al. 1987). Furthermore, these terminal complexes were reported to extend into the plasma membrane somewhat deeper than the neighboring cortical microtubules. In the present study, the terminal complexes also appear to be taller (i.e., extend deeper into the cytoplasm) than the adjacent microtubules (e.g., Fig. 7D). Pristine, in vitro polymerized microtubules are known to be 24 nm in diameter by X-ray crystallography; however, the microtubules imaged in the current study are somewhat larger than this due to the presence of the various microtubule-associated proteins which are present in living cells. Therefore, the height of the cytoplasmic domain of the rosette terminal complex in tobacco BY-2 cells is probably very similar to the 35 nm height of the linear terminal complexes seen in *B. forbesii* by Kudlicka et al. (1987). It is possible, however, that the cortical microtubules may have settled onto the surface of the coverslip upon extraction of the plasma membrane lipids, while the terminal complexes, which extend through the plasma membrane and therefore would not settle as the membrane is removed, did not. This would add 4–5 nm (the thickness of the plasma membrane) onto the appar-

ent height of the terminal complexes, such that their true height may be closer to 30 nm. The actual height of the terminal complexes is therefore likely to be between 30 and 35 nm from the inner surface of the plasma membrane.

#### *Nonhexagonal terminal complexes*

The cytoplasmic regions of some terminal complexes do not have any apparent hexagonal symmetry and are highly variable in structure (Fig. 9). Perhaps the most likely explanation of this nonhexagonal morphology is that these terminal complexes are in the process of being broken down and/or inactivated. The particles composing these terminal complexes could be proteolytically cleaved portions of the terminal complex (Nakashima et al. 2003). These disrupted, partially degraded terminal complexes may aggregate but retain some members still bound to the microfibril tip. Terminal complexes have been reported to have a very short half-life (Rudolph et al. 1989). In fact, in the moss *Funaria hygrometrica*, large percentages (20%) of rosette terminal complexes were observed to be in a nonrosette conformation (Reiss et al. 1984). The authors' conclusion was that these terminal complexes may represent disintegrating or aggregating terminal complexes. Furthermore, that study used quick-freeze followed by freeze fracture, where the specimen disturbance during preparation would be minimal. Thus it seems likely that the nonhexagonal images shown in the current study are not an artifact of the specimen preparation technique, although this cannot be completely ruled out.

Alternatively, this variable morphology may be indicative of the presence of various adapter proteins associated with the cytoplasmic face of the terminal complexes (Delmer 1999, Somerville et al. 2004). These adapter proteins may attach to the cytoplasmic face of the terminal complex and modify its behavior. One example of a protein that might be associated with the cytoplasmic domain of the terminal complex is sucrose synthase (Amor et al. 1995, Salnikov et al. 2001). The sonication may in some cases remove noncovalently bound proteins, thus exposing the hexagonal shape of the underlying cellulose-synthetic apparatus, while in other cases, the noncovalently bound proteins may remain attached to the terminal complex, obscuring the hexagonal shape. It should also be mentioned that it is possible that these are an artifact of the rather violent specimen generation process or they may be some type of unrelated cellular debris.

#### *Effect of secondary and tertiary fixations on plasma membrane sheet ultrastructure and cellulose synthases*

Both osmium tetroxide and uranyl acetate are well known lipid fixatives (Glauert and Lewis 1998). The inclusion of both of these lipid-specific fixatives greatly enhances the preservation of the plasma membrane; therefore, the increased preservation of the ultrastructure of the clathrin-coated vesicles is not surprising. In fact, the surface of the plasma membrane of the specimens shown in Fig. 3 is very similar to what has been seen in animal cells (Aggeler and Werb 1982, Heuser 2000) and plant cells (Grout 1975, Willison and Cocking 1975, Williamson et al. 1977) using the quick-freeze-deep-etch technique. However, for the current study, the increased preservation of the plasma membrane is a disadvantage because it precludes any direct correlation between cytoplasmic and extracellular structures. Only when the plasma membrane is partially extracted can cellulose microfibrils be discerned beneath the plasma membrane sheet.

#### *Can microtubules guide terminal complexes (or vice versa)?*

The cytoplasmic domain of terminal complexes can be seen to protrude from the inner surface of the plasma membrane farther than neighboring cortical microtubules. Furthermore, a tight association between cortical microtubules and the plasma membrane can be inferred from the fact that these structures remain attached to the plasma membrane after sonication, which should remove all loosely bound cellular material. Thus, it seems reasonable to conclude that these microtubules and terminal complexes have the ability to interact with and orient each other.

One recent report has shown that fluorescently labeled terminal complexes follow microtubule tracks along the inner surface of the plasma membrane in intact plant cells (Paredes et al. 2006). Due to the high degree of spatial and temporal association between terminal complexes and cortical microtubules, especially so-called discordant and curved microtubules, the authors concluded that the cytoplasmic domain of terminal complexes associates directly with microtubules. While some evidence of parallel cortical microtubules and extracellular cellulose microfibrils was observed on plasma membrane sheets (data not shown), arrays of terminal complexes tracking along microtubules were not observed. Although the current data seem to support the theory that terminal complexes are bracketed between microtubule guide-rails (Giddings and

Stahelin 1991), and not continuously bound to them, there are several reasons why this conclusion cannot be made from the data presented herein.

*Possible implications of the hexagonal morphology and the relatively large observed size of the cytoplasmic domain of the terminal complex*

An analysis of proteins of different cross-sectional areas has revealed that a linear relationship exists between the number of trans-membrane alpha-helices of a protein and the size of the cross-sectional area on freeze-fracture replicas (Eskandari et al. 1998). The area contributed by an individual alpha-helical transmembrane domain is 1.40 nm<sup>2</sup> (Eskandari et al. 1998). The diameter of the subunits of the rosette terminal complex determined by UHV freeze fracture is 8 nm (Reiss et al. 1984, Rudolph and Schnepf 1988, Rudolph et al. 1989). The area of an 8 nm circle is 50.3 nm<sup>2</sup>. The area of 36 alpha helices is 50.4 nm<sup>2</sup>. Therefore, the presence of as many as 36 transmembrane alpha-helices is theoretically possible in this area. Six transmembrane helices are predicted at the COOH terminus of CesaA proteins and two are predicted at the N terminus (Pear et al. 1996, Arioli et al. 1998, Doblin et al. 2002). If each CesaA molecule has 8 transmembrane regions, then perhaps each subunit of the rosette contains 4 CesaA proteins (32 transmembrane regions, or 44.8 nm<sup>2</sup>), with the "extra" area due to the presence of a central pore for cellulose mini-sheets to move through to the outside of the cell. The observed size of the cytoplasmic region of the terminal complex is consistent with the presence of this number of CesaA proteins. Furthermore, the relatively large size of the cytoplasmic domain of the terminal complex strongly suggests that other proteins besides just CesAs are associated with the terminal complex in vivo.

*Conclusions*

The cell ghost-cortex isolation technique has been refined specifically for imaging the cytoplasmic domains of transmembrane proteins and correlating these structures with extracellular landmarks. This involves both the stripping of cytoplasmic proteins by sonication and the partial extraction of membrane lipids by the omission of lipid fixatives coupled with dehydration in ethanol. This technique was used to visualize the cytoplasmic domain of rosette terminal complexes in plasma membrane sheets isolated from tobacco BY-2 cells. Rosette terminal complexes were identified on the basis of their association with the

termini of cellulose microfibrils. Although a cytoplasmic component has been predicted by the sequence of the CesaA protein, this is the first direct evidence supporting the hypothesis that rosette terminal complexes have a substantial cytoplasmic domain. The cytoplasmic domain of the rosette terminal complex was shown to be hexagonal in shape, mirroring the shape of the transmembrane region seen by freeze fracture. The size of the hexagonal terminal complex was shown to be 45–50 nm in diameter and the height of the hexagonal particles was estimated to be approximately 30–35 nm. The relatively large size of the cytoplasmic component of the terminal complex is compatible with the existence of multiple types of terminal complex-associated proteins. Images of terminal complexes composed of multiple subunits were also seen and are thought to be terminal complexes in the process of inactivation, on the basis of previous sightings of analogous structures in freeze-fracture specimens.

**References**

- Aggeler J, Werb Z (1982) Initial events during phagocytosis by macrophages viewed from outside and inside the cell – membrane-particle interactions and clathrin. *J Cell Biol* 94: 613–623
- Amor Y, Haigler CH, Johnson S, Wainscott M, Delmer DP (1995) A membrane-associated form of sucrose synthase and its potential role in synthesis of cellulose and callose in plants. *Proc Natl Acad Sci USA* 92: 9353–9357
- Amos L (2000) Focusing-in on microtubules. *Curr Opin Struct Biol* 10: 236–241
- Arioli T, Peng LC, Betzner AS, Burn J, Wittke W, Herth W, Camilleri C, Hofte H, Plazinski J, Birch R, Cork A, Glover J, Redmond J, Williamson RE (1998) Molecular analysis of cellulose biosynthesis in *Arabidopsis*. *Science* 279: 717–720
- Bradley DE (1965) Replica and shadowing techniques. In: Kay DH (ed) *Techniques for electron microscopy*, 2nd edn. Blackwell, Oxford, pp 96–97
- Branton D, Bullivant S, Gilula N (1975) Freeze etching nomenclature. *Science* 190: 54–56
- Brown RM Jr (1996) The biosynthesis of cellulose. *J Macromol Sci Pure Appl Chem* A33: 1345–1373
- Brown RM Jr, Montezinos D (1976) Cellulose microfibrils: visualization of biosynthetic and orienting complexes in association with the plasma membrane. *Proc Natl Acad Sci USA* 73: 143–147
- Delmer DP (1999) Cellulose biosynthesis: exciting times for a difficult field of study. *Annu Rev Plant Physiol Plant Mol Biol* 50: 245–276
- Doblin MS, Kurek I, Jacob-Wilk D, Delmer DP (2002) Cellulose biosynthesis in plants: from genes to rosettes. *Plant Cell Physiol* 43: 1407–1420
- Eskandari S, Wright EM, Kreman M, Starace DM, Zampighi GA (1998) Structural analysis of cloned plasma membrane proteins by freeze-fracture electron microscopy. *Proc Natl Acad Sci USA* 95: 11235–11240
- Giddings TH Jr, Stahelin LA (1991) Microtubule-mediated control of microfibril deposition: a re-examination of the hypothesis. In: Lloyd CW (ed) *The cytoskeletal basis of plant growth and form*. Academic Press, London, pp 85–99
- Giddings TH Jr, Brower DL, Stahelin LA (1980) Visualization of particle complexes in the plasma membrane of *Micrasterias denticulata*

- associated with the formation of cellulose fibrils in primary and secondary cell walls. *J Cell Biol* 84: 327–329
- Glauert A, Lewis P (1998) Biological specimen preparation for transmission electron microscopy. Princeton University Press, Princeton, NJ
- Grout BWW (1975) Cellulose microfibril deposition at the plasmalemma surface of regenerating tobacco mesophyll protoplasts: a deep-etch study. *Planta* 123: 275–282
- Herth W (1983) Arrays of plasma membrane “rosettes” in cellulose microfibril formation of *Spirogyra*. *Planta* 159: 347–356
- Heuser J (2000) The production of ‘cell cortices’ for light and electron microscopy. *Traffic* 1: 545–552
- Hirai N, Sonobe S, Hayashi T (1998) In situ synthesis of  $\beta$ -glucan microfibrils on tobacco plasma membrane sheets. *Proc Natl Acad Sci USA* 95: 15102–15106
- Kimura S, Laosinchai W, Itoh T, Cui X, Linder CR, Brown RM Jr (1999) Immunogold labeling of rosette terminal cellulose-synthesizing complexes in the vascular plant *Vigna angularis*. *Plant Cell* 11: 2075–2085
- Kudlicka K, Wardrop A, Itoh T, Brown RM Jr (1987) Further evidence from sectioned material in support of the existence of a linear terminal complex in cellulose synthesis. *Protoplasma* 136: 96–103
- Marchant HJ (1978) Microtubules associated with the plasma membrane isolated from protoplasts of the green alga *Mougeotia*. *Exp Cell Res* 115: 25–30
- Markham R, Frey S, Hills GJ (1963) Methods for the enhancement of image detail and accentuation of structure in electron microscopy. *Virology* 20: 88–102
- Mazia D, Schatten G, Sale W (1975) Adhesion of cells to surfaces coated with polylysine: applications to electron microscopy. *J Cell Biol* 66: 198–200
- Mueller SC, Brown RM Jr (1980) Evidence for an intramembrane component associated with a cellulose microfibril synthesizing complex in higher plants. *J Cell Biol* 84: 315–326
- Nagata T, Kumagai F (1999) Plant cell biology through the window of the highly synchronized tobacco BY-2 cell line. *Methods Cell Sci* 21: 123–127
- Nakashima J, Laosinchai W, Cui XJ, Brown RM Jr (2003) New insight into the mechanism of cellulose and callose biosynthesis: proteases may regulate callose biosynthesis upon wounding. *Cellulose* 10: 369–389
- Nogales E, Whittaker M, Milligan RA, Downing KH (1999) High-resolution model of the microtubule. *Cell* 96: 79–88
- Paredez AR, Somerville CR, Ehrhardt DW (2006) Visualization of cellulose synthase demonstrates functional association with microtubules. *Science* 312: 1491–1495
- Pear JR, Kawagoe Y, Schreckengost WE, Delmer DP, Stalker DM (1996) Higher plants contain homologs of the bacterial *celA* genes encoding the catalytic subunit of cellulose synthase. *Proc Natl Acad Sci USA* 93: 12637–12642
- Perrin RM (2001) Cellulose: how many cellulose synthases to make a plant? *Curr Biol* 11: R213–R216
- Reiss HD, Schnepf E, Herth W (1984) The plasma-membrane of the *Funaria caulonema* tip cell – morphology and distribution of particle rosettes, and the kinetics of cellulose synthesis. *Planta* 160: 428–435
- Robards AW (1969) Particles associated with developing plant cell walls. *Planta* 88: 376–379
- Roelofsens A (1958) Cell wall structure as related to surface growth. *Acta Bot Neerl* 7: 77–89
- Roland JC, Vian B (1991) General preparation and staining of thin sections. In: Hall JL, Hawes C (eds) *Electron microscopy of plant cells*. Academic Press, New York, pp 1–66
- Rudolph U, Schnepf E (1988) Investigations of the turnover of the putative cellulose-synthesizing particle rosettes within the plasma membrane of *Funaria hygrometrica* protonema cells. 1. Effects of monensin and cytochalasin B. *Protoplasma* 143: 63–73
- Rudolph U, Gross H, Schnepf E (1989) Investigations of the turnover of the putative cellulose-synthesizing particle rosettes within the plasma membrane of *Funaria hygrometrica* protonema cells. 2. Rosette structure and the effects of cycloheximide, actinomycin-D, 2,6-dichlorobenzonitrile, Biofluor, heat-shock, and plasmolysis. *Protoplasma* 148: 57–69
- Salnikov VV, Grimson MJ, Delmer DP, Haigler CH (2001) Sucrose synthase localizes to cellulose synthase sites in tracheary elements. *Phytochemistry* 57: 823–833
- Somerville C, Bauer S, Brininstool G, Facette M, Hamann T, Milne J, Osborne E, Paredez A, Persson S, Raab T, Vorwerk S, Youngs H (2004) Toward a systems approach to understanding plant cell walls. *Science* 306: 2206–2211
- Van der Valk P, Fowke LC (1981) Ultrastructural aspects of coated vesicles in tobacco protoplasts. *Can J Bot* 59: 1307–1313
- Van der Valk P, Rennie PJ, Connolly JA, Fowke LC (1980) Distribution of cortical microtubules in tobacco protoplasts – an immunofluorescence microscopic and ultrastructural study. *Protoplasma* 105: 27–43
- Williamson FA, Fowke LC, Weber G, Constabel F, Gamborg O (1977) Microfibril deposition on cultured protoplasts of *Vicia hajastana*. *Protoplasma* 91: 213–219
- Willison JHM, Cocking EC (1975) Microfibril synthesis at the surfaces of isolated tobacco mesophyll protoplasts, a freeze-etch study. *Protoplasma* 84: 147–159
- Willison JHM, Rowe AJ (1980) Replica, shadowing and freeze-etching techniques. In: Glauert AM (ed) *Practical methods in electron microscopy*, vol 8. North-Holland, Amsterdam, pp 171–244